Mineralogical Magazine, October 2012, Vol. 76(5), pp. 1247–1255

Rumseyite, $[Pb_2OF]Cl$, the first naturally occurring fluoroxychloride mineral with the parent crystal structure for layered lead oxychlorides

R. W. Turner[1,*], O. I. Siidra[2], S. V. Krivovichev[2], C. J. Stanley[3] and J. Spratt[3]

[1] The Drey, Allington Track, Allington, Salisbury, Wiltshire SP4 0DD, UK
[2] Department of Crystallography, Geological Faculty, St Petersburg State University, University Embankment 7/9, St Petersburg 199034, Russia
[3] Department of Earth Sciences, Natural History Museum, Cromwell Road, London SW7 5BD, UK

[*Received 21 March 2012; Accepted 10 August 2012; Associate Editor: G. Diego Gatta*]

ABSTRACT

Rumseyite, ideally $[Pb_2OF]Cl$, is a new mineral species which is associated with calcite, cerussite, diaboleite, hydrocerussite and undifferentiated Mn oxides in a small cavity in 'hydrocerussite' from a manganese pod at Merehead quarry, Somerset, England. Rumseyite is tetragonal, $I4/mmm$, a = 4.065(1), c = 12.631(7) Å, V = 208.7(1) Å^3, Z = 2. The mineral is translucent pale orange-brown with a white streak and vitreous lustre. It is brittle with perfect {100} cleavage; D_{calc} = 7.71 g cm^{-3} (for the ideal formula, $[Pb_2OF]Cl$). The mean refractive index in air at 589 nm is 2.15. The six strongest reflections in the X-ray powder-diffraction pattern [d_{meas} in Å, (I_{rel}), (hkl)] are as follows: 2.923(100)(013), 2.875(68)(110), 3.848(41)(011), 6.306(17)(002), 1.680(14)(123), 2.110(12)(006). The crystal structure of rumseyite is based on alternating $[OFPb_2]$ and Cl layers. Rumseyite is related to other layered Pb oxyhalides. Fluorine and oxygen are statistically disordered over one crystallographic site. Rumseyite is named in honour of Michael Scott (Mike) Rumsey (1980–), Curator and Collections Manager at the NHM (London), who discovered the mineral. The mineral and name have been approved by the IMA Commission on New Mineral Names and Classification (IMA 2011-091). The holotype specimen is in the collections of the Natural History Museum, London (specimen number BM1970,110).

Keywords: rumseyite, Merehead quarry, Mendip Hills, layered lead oxychlorides, lead oxyhalides, new mineral species.

Introduction

For some time we have been investigating the mineralogy of the Mendip Hills with particular reference to the assemblages of Pb oxyhalides and other Pb secondary minerals in the manganese pods that occur there; we have also investigated similar oxyhalide minerals from elsewhere in the world (e.g. Turner, 2006; Rumsey, 2008; Siidra and Krivovichev, 2008; Siidra *et al*., 2008*a*,*b*; Krivovichev *et al*., 2009; Turner and Rumsey, 2010; Rumsey *et al*., 2011; Turner *et al*., 2012). In the course of this research, specimens in the collections of the Natural History Museum (NHM), London were examined, and one was found to contain an unusual looking phase, which subsequently proved to be the new mineral rumseyite. The mineral and name have been approved by the IMA Commission on New Mineral Names and Classification (IMA 2011-091). The holotype specimen is stored in the collections of the NHM under catalogue number BM1970,110. Rumseyite is named in

* E-mail: rturner@imbuia-holdings.com
DOI: 10.1180/minmag.2012.076.5.11

honour of the discoverer, Michael Scott (Mike) Rumsey (1980–), Curator and Collections Manager at the Natural History Museum. Mike is noted for his work on the mineralogy of the Mendip Hills and Kombat mine (Namibia), and in particular for studies of Pb oxychlorides and related Pb secondary minerals, which have already led to the description of several new minerals (Rumsey *et al*., 2011; Turner *et al*., 2012).

Occurrence

Rumseyite is an extremely rare constituent of a lead-dominated mineral assemblage which occurs in manganese oxide pods irregularly distributed in Carboniferous Limestone at the Merehead (also known as Torr Works) quarry, East Cranmore, Somerset, England.

The origin of the manganese oxide pods and the lead oxychloride phases that they enclose has been debated for many years. Turner (2006) suggested that the lead oxychlorides formed when galena was locally exposed to the action of seawater. Surface oxidation of the galena initiated the deposition of manganese minerals, which adsorbed heavy metals from the seawater and the local environment. A later hydrothermal event caused the galena to decompose, a variety of secondary minerals to form and the conversion of the manganate phases to manganese oxides. These oxides formed an impervious layer around a lead-rich core and generated a series of closed systems (the manganese pods). The chemistry of these systems is dependent on local starting conditions, and there is considerable variation in mineralogy from one manganese pod to another.

Associated minerals are calcite, cerussite, diaboleite, 'hydrocerussite' and undifferentiated Mn oxides, typically a mixture of manganite and pyrolusite (Turner, 2006). It has been shown that the so-called 'hydrocerussite' from this locality is made up of a number of different phases, which at the time of this submission still require further characterization (Turner and Rumsey, 2010); the term hydrocerussite is used *sensu lato* in the following text.

Rumseyite is in direct contact only with hydrocerussite on the type specimen, although there are a small number of minute diaboleite crystals nearby. The hydrocerussite mass containing the rumseyite is coated with a rind of cerussite, and lies within a cavity in a typical pyrolusite-, manganite- and calcite-rich pod.

Appearance

Rumseyite is currently known from a single cavity, ~1.5 × 1 × 1 mm in size, on the holotype specimen, where it is enclosed in a platy mass of hydrocerussite (Figs 1–3); it is possible that other examples will be identified as similar hydrocerussite specimens were abundant at the time that this specimen was collected and added to the NHM collection. They can be identified by their characteristic foliated appearance, off-white colour with a distinct greenish tinge, and pearly lustre. Rumseyite does not completely fill the cavity but is nucleated into one main crystalline mass, with a few other small crystals and crystalline fragments adhering to the cavity edges and nearby fractures in the hydrocerussite crystal. In the unfilled portion of the cavity, platy sheaves of hydrocerussite coat rumseyite and the cavity walls. Sparse diaboleite occurs but only in direct contact with hydrocerussite.

Rumseyite forms an irregular crystalline mass (Fig. 2) which scanning electron microscope (SEM) examination shows to be composed of aggregates of minute tabular to prismatic crystallites with pyramidal terminations (Fig. 3). No twinning has been observed. The small size of the micro crystals precludes direct measurement but they show forms that appear to be {100} prisms, with {111} pyramid and rarely, small {001} pinacoid terminations.

FIG. 1. The whole of the holotype specimen of rumseyite (BM 1970,110), showing platy white hydrocerussite on a typical manganese oxide matrix. The specimen is ~40 mm across. Rumseyite is the small square pinkish brown patch just above and right of centre.

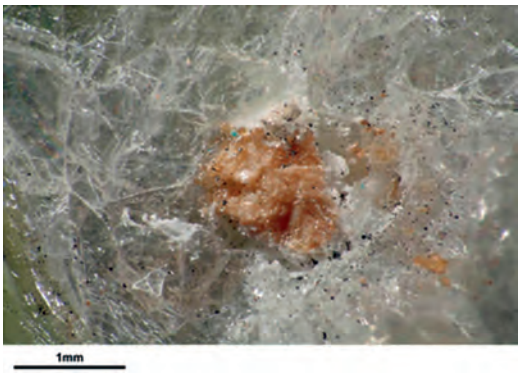

FIG. 2. Part of the holotype specimen (BM 1970,110) of rumseyite showing the approximately cuboidal mass of rumseyite in hydrocerussite. Small pale blue crystals of diaboleite are also present.

Terminated rumseyite crystals in the main aggregate are generally no larger than about $50 \times 50 \times 100$ μm, and most are much smaller, typically ~$15 \times 15 \times 30$ μm. Broken surfaces within the aggregate suggest that it might be composed of a small number of larger intergrown but heavily fractured and poorly formed crystals without terminations, in which case the largest crystal size would have been in the range 100 to 500 μm. A single, well-formed, possibly double terminated crystal, $250 \times 80 \times 80$ μm in size, that was not attached to the main mass, was removed and used for single-crystal and powder-diffraction analysis.

FIG. 3. Scanning electron microscope showing minute tetragonal crystals of rumseyite with conspicuous prism and pyramid faces and small rare pinacoids.

Physical properties

Rumseyite is translucent pale orange-brown with a white streak and vitreous lustre. It is brittle with perfect {100} cleavage, no observed parting and a conchoidal fracture. Hardness and density could not be measured due to lack of material. The calculated density for the ideal formula $[Pb_2OF]Cl$ is 7.72 g cm^{-3}.

Optical properties

Rumseyite is non-metallic, but has the high refractive index (RI) typical of lead oxychlorides. Its optical properties were studied using the methods common for metallic minerals to avoid using toxic RI liquids. In reflected light rumseyite is grey with abundant pale yellow internal reflections; it is not pleochroic and has no bireflectance. Any anisotropy is masked by the internal reflections. Reflectance values are listed in Table 1. The mean RI in air at 589 nm calculated from the Fresnel Equation (assuming $k = 0$) is 2.15, which is similar to other Pb oxychloride minerals.

Chemical composition

Twenty-five chemical analyses were obtained using a Cameca SX100 electron microprobe operating in wavelength-dispersive spectrometry (WDS) mode at 20 kV and 20 nA with a 1 μm beam diameter. Analytical results and standards are listed in Table 2; Mo, As, Cr, V, P and Mg were sought, but they were below detection limits. No other elements were detected by energy-dispersive spectrometry (EDS) on a Jeol 5900LV variable pressure scanning electron microscope. Insufficient material exists for the determination of H_2O or CO_2 by CHN analysis.

The possible presence of borate or carbonate groups, which are known in some Pb oxychloride minerals from this area (e.g. Welch *et al*., 1998; Krivovichev *et al*., 2009) was ruled out by the structure determination. The absence of carbonate was also indicated by a preliminary uncoated EDX analysis.

In the data reduction, O was determined by difference rather than by stoichiometry. The reason for this is the presence of F and Cl, which would have resulted in an excess of O of ~3 wt.% in the PAP matrix correction. This excess O would result in an overcorrection, particularly to the F data, due to the large

TABLE 1. Reflectance values on an area of 10 × 10 μm of an unoriented section of rumseyite with no internal reflections (using a SiC standard, measured in air).

λ (nm)	*R* (%)
400	15.6
420	15.3
440	15.0
460	14.7
470 (COM)	**14.6**
480	14.4
500	14.1
520	13.9
540	13.7
546 (COM)	**13.6**
560	13.5
580	13.4
589 (COM)	**13.4**
600	13.3
620	13.2
640	13.2
650 (COM)	**13.2**
660	13.2
680	13.3
700	13.5

The COM wavelengths and reflectances, listed in bold, are those recommended by the Commission on Ore Microscopy.

absorption correction made to F in the presence of O. The O value was subsequently calculated by stoichiometry, and this value is quoted in Table 2. The O wt.% value used in the matrix correction is thus ((100 − total) + stoichiometric O wt.%) which produces an overestimation of O in the matrix correction of less than 1 wt.%.

The possibility that hydroxyl groups might partly substitute for O and F was ruled out on the basis of structural and crystal-chemical considerations. Any OH group present would either have to replace the central *X* atom in an anion-centred *X*Pb4 (*X* = O, F) tetrahedron, which is not chemically possible; or to replace Cl in chlorine sites in the interlayer; although this is possible, these sites were found to be fully occupied by Cl in the structure refinement.

The empirical charge-balanced formula for rumseyite, based on the data in Table 2, is $Pb_{2.039}O_{1.00}F_{0.992}Cl_{1.001}$, and the ideal formula is $[Pb_2OF]Cl$, which requires PbO 92.07, Cl 7.31, F 3.92, O = F + Cl −3.30; total 100.00 wt.%.

X-ray diffraction data

A fragment of the 250 × 80 × 80 μm crystal that was removed from the specimen was used for single-crystal structure analysis. It was mounted on a Stoe IPDS II diffractometer operated at 50 kV and 40 mA at the Department of Crystallography, St Petersburg State University, Russia. More than a hemisphere of three-dimensional data was collected using monochromatic Mo*K*α radiation, with frame widths of 2° in ω, and a 600 s count for each frame. Unit-cell parameters (Table 3) were refined using least-squares techniques. The analysis revealed tetragonal symmetry, *I*4/*mmm*, a = 4.065(1), c = 12.631(7) Å, V = 208.7(1) Å^3, Z = 2. The intensity data were integrated and corrected for Lorentz, polarization and background effects using the Stoe program *X-Area*. An analytical absorption correction based on the indexed faces was applied. The structure of rumseyite was refined to R_1 = 0.072 for 64 unique reflections with $F^2 \geqslant 4\sigma(F^2)$, using the simplified formula, indicating the lack of defects in the Pb−O−F sheet. Every relevant atom position is filled either

TABLE 2. Analytical data for rumseyite.

Constituent	Mean (wt.%)	Range	SD	Standard
PbO	91.63	90.73−92.44	0.37	Vanadinite
F	3.53	3.05−3.75	0.17	Topaz
Cl	7.15	6.89−7.33	0.10	Vanadinite
O = F + Cl	−3.23			
Total	99.08			

TABLE 3. Crystallographic data and refinement parameters for rumseyite.

Crystal data	
Temperature (K)	293
Radiation, wavelength (Å)	Mo$K\alpha$, 0.71073
Crystal system	tetragonal
Space group	$I4/mmm$
Unit-cell dimensions a, c (Å)	4.065(1), 12.631(7)
Unit-cell volume (Å^3)	208.7(1)
Z	2
Calculated density (g cm^{-3})	7.72
Absorption coefficient (mm^{-1})	81.038
Data collection	
θ range (º)	6.98–27.83
h, k, l ranges	$0 \rightarrow 3$, $0 \rightarrow 5$, $0 \rightarrow 16$
Total reflections collected	93
Unique reflections $F > 4\sigma(F)$	64
Structure refinement	
Refinement method	Full-matrix least-squares on F^2
Weighting coefficients a, b	0.1323, 0.0
Extinction coefficient	0.003(5)
Data/restraints/parameters	873/0/47
R_1 [$F > 4\sigma(F)$], wR_2 [$F > 4\sigma(F)$],	0.071, 0.202
R_1 (all), wR_2 (all)	0.099, 0.215
Goodness-of-fit on F^2	1.107
Largest diff. peak and hole (e Å^{-3})	2.90, −2.37

with O or F, and there are no vacancies in the sheet. This contrasts with every other natural litharge-derived Pb-oxyhalide.

The poor quality of the crystal resulted in relatively a high R_1 factor and high displacement parameters (Table 4). These are typical of Pb-oxyhalide minerals, which do not commonly form crystals of the perfection required for high resolution single-crystal X-ray studies (e.g. Cooper and Hawthorne, 1994; Welch *et al.*, 1998; Pasero and Vacchiano, 2000). The best possible crystal fragment was chosen for examination from the tiny amount of material that was available. Final atom coordinates and anisotropic-displacement parameters are given in Table 4. A list of observed and calculated structure factors has been deposited with *Mineralogical Magazine* and can be downloaded from http://www.minersoc.org/pages/e_journals/dep_mat_mm.html.

X-ray powder diffraction data were obtained using a STOE STADI P diffractometer at the Department of Crystallography, St Petersburg State University, Russia after crushing the crystal fragment used for the single crystal

TABLE 4. Atom coordinates, site occupancies and displacement parameters (Å^2) for rumseyite.

Site	Wyckoff position	Occupancy	x/a	y/a	z/c	U_{eq}	U_{11}	U_{22}	U_{33}
Pb	4e	1	0	0	0.1469(3)	0.061(2)	0.065(2)	0.065(2)	0.052(2)
Cl	2b	1	½	½	0	0.056(7)	0.062(11)	0.062(11)	0.043(14)
OF	4d	$O_{0.5}F_{0.5}$	½	0	¼	0.049(11)	0.049(17)	0.049(17)	0.05(2)

The off-axis tensor components, U_{12}, U_{13} and U_{23} = 0.

analysis (there being insufficient additional material for another sample, and it also being necessary to preserve as much as possible of the holotype specimen for future study). These data are listed in Table 5. Refinement in the tetragonal space group *I*4/*mmm* produced $a = 4.07(1)$ Å, $c = 12.61(1)$ Å, $V = 208.4(1)$ Å^3, with $Z = 2$, which is in excellent agreement with the single-crystal data.

Crystal structure

The structure of rumseyite contains one crystallographically unique Pb position. The Pb^{2+} cation is coordinated by four O/F atoms and four Cl atoms. The Pb^{2+} cations in rumseyite are coordinated by short Pb−O/F bonds (2.41 Å) in one coordination hemisphere (Fig. 4); in the opposite hemisphere there are four long Pb−Cl bonds (3.42 Å). This distortion, which is a general feature of Pb-oxychlorides, is usually interpreted as being due to the influence of the stereoactivity of s^2 lone electron pairs on the Pb^{2+} cations. The coordination geometry of the Pb atom in rumseyite can be described as a distorted square antiprism. The Cl atoms have cubic coordination, whereas the O/F atoms have tetrahedral coordination, thus being central for anion-centred $(O/F)Pb_4$ tetrahedra. The presence of fluorine in the crystal structure of rumseyite is confirmed by the Pb−(O/F) bond length of 2.41 Å. The mean bond length for ideal OPb_4 tetrahedra is 2.33 Å (Krivovichev and Filatov, 1999). Anion-centred FPb_4 tetrahedra are present in grandreefite, $Pb_2F_2(SO_4)$ (Kampf, 1991). The average Pb−F bond length in this structure is 2.55 Å, with individual bond lengths in the range 2.39−2.71 Å.

The crystal structure of rumseyite is based on an alternation (Fig. 5) of continuous $[OFPb_2]$ layers of edge-sharing XPb_4 tetrahedra (X = O, F; Fig. 6*a*) and sheets of chloride ions (Fig. 6*c*). The $[OFPb_2]$ layers are of the type observed in the structure of tetragonal PbO (Dickinson and Friauf, 1924). Note that the unit-cell parameters and the structural motif are very similar to those of a related synthetic lead oxychloride described by Gasperin (1964).

TABLE 5. Powder X-ray data for rumseyite.

I_{rel} (%)	d_{meas} (Å)	d_{calc} (Å)	h	k	l
17	6.306	6.316	0	0	2
41	3.848	3.869	0	1	1
4	3.149	3.158	0	0	4
100	2.923	2.924	0	1	3
68	2.875	2.874	1	1	0
12	2.110	2.105	0	0	6
10	2.049	2.032	0	2	0
9	1.719	1.709	0	2	4
14	1.680	1.669	1	2	3
3	1.646	1.649	0	1	7
2	1.440	1.437	2	2	0
3	1.281	1.281	1	2	7

Data acquired using MoKα radiation.

Discussion

The rumseyite structure is closely related to a number of other Pb-oxyhalide minerals with litharge-like sheets. The PbO-like sheets in all of these minerals are made up of edge- and corner-sharing OPb_4 oxocentred tetrahedra and/or halide layers; however, all of the other minerals have different types of vacancies in the sheets. For instance, the defects in the PbO-like layers in the structure of symesite have a square form (Fig. 6*b*). In mereheadite, additional Pb atoms are inserted in the chloride layer (Fig. 6*d*). This leads us to conclude that the crystal structure of rumseyite is a defect-free parent of all of the minerals in the growing class of layered lead oxychlorides. Interestingly, the structure of rumseyite is the same as that of perite (Gillberg, 1960) and nadorite (Giuseppetti and Tadini, 1973), but the oxocentred layers in perite and nadorite are made up of OPb_2A_2 (A = Bi, Sb) heterometallic tetrahedra (Siidra *et al.*, 2008*a*). This makes rumseyite very different from these

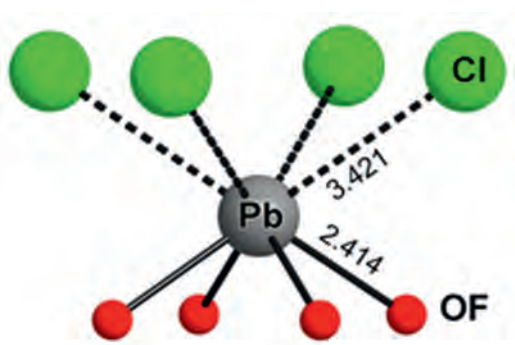

FIG. 4. Coordination of the Pb^{2+} cation in rumseyite.

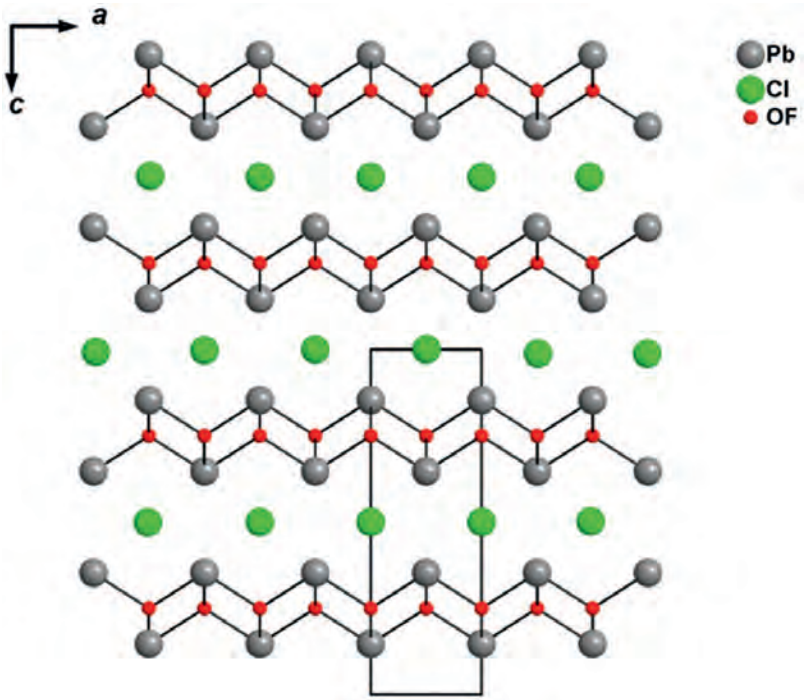

FIG. 5. Projection of the crystal structure of rumseyite along the *b* axis. The Pb−Cl bonds are omitted for clarity.

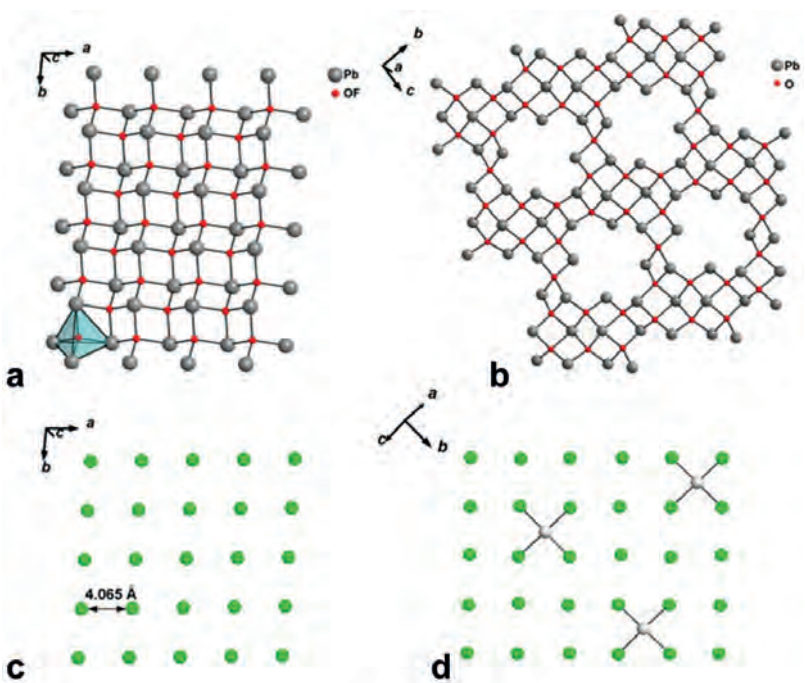

FIG. 6. (*a*) Projection of the [$OFPb_2$] layer and (*c*) the chloride layer in rumseyite. (*b*) The PbO-like sheet with square vacancies in the crystal structure of symesite and (*d*) Pb atoms inserted into the halide sheet in mereheadite.

minerals; it is the first Pb oxychloride mineral containing defect-free halide and PbO-like layers. Lead oxychlorides with layered defect-free PbO-derived blocks were first described in synthetic compounds by Aurivillius (1982, 1983) but rumseyite is the first example of mineral with this type of atomic arrangement.

Rumseyite is also the first example of a mineral crystal structure containing mixed O/F anion-centred tetrahedra. The fluoride anion plays an important role as a charge compensating agent within the O–Pb sheets. As F and O have similar electron densities, they are difficult to distinguish by single-crystal XRD; an attempt was made to refine the occupancy of unique sites for oxygen and fluorine in order to assign rumseyite to a lower symmetry space group. However, no indication of lower symmetry was found. The data were also checked using the *PLATON* computer program to verify these findings.

Rumseyite appears to have formed in a highly unusual environment as fluorine is otherwise absent from the manganese pod mineral assemblages. The only fluorine-bearing mineral present in the Mendips is fluorite, which is widespread but scarce in the original primary galena-bearing veins. It is possible that a small trapped fluorite crystal was the original source of the fluorine in rumseyite.

Acknowledgements

This work was supported (OIS and SVK) through a President of the Russian Federation grant for young scientists (# MK-5074.2011.5) (OIS), an internal grant (3.38.83.2012) and by X-ray Diffraction Resource Centre of St Petersburg State University.

References

Aurivillius, B. (1982) On the crystal structure of a number of non-stoichiometric mixed lead oxide halides composed of PbO like blocks and single halogen layers. *Chemica Scripta*, **19**, 97–107.

Aurivillius, B. (1983) On the crystal structure of some non-stoichiometric mixed lead oxide halides and their relation to the minerals "lorettoite" and sundiusite. *Chemica Scripta*, **22**, 5–11.

Cooper, M.A. and Hawthorne, F.C. (1994) The crystal structure of kombatite, $Pb_{14}(VO_4)_2O_9Cl_4$, a complex heteropolyhedral sheet mineral. *American Mineralogist*, **79**, 550–554.

Dickinson, R.G. and Friauf, J.B. (1924) The crystal structure of tetragonal lead monoxide. *Journal of the American Chemical Society*, **46**, 2457–2462.

Gasperin, M. (1964) Sur la synthese d'un oxychlorure de plomb. *Bulletin de la Société française de Minéralogie et de Cristallographie*, **87**, 278–280.

Gillberg, M. (1960) Perite, a new oxyhalide mineral from Långban, Sweden. *Arkiv för Mineralogi och Geologi*, **2**, 565–570.

Giuseppetti, G. and Tadini, C. (1973) Riesame della struttura cristallina della nadorite: $PbSbO_2Cl$. *Periodico di Mineralogia*, **42**, 335–345.

Kampf, A.R. (1991) Grandreefite, $Pb_2F_2SO_4$: crystal structure and relationship to the lanthanide oxide sulfates, $Ln_2O_2SO_4$. *American Mineralogist*, **76**, 278–282.

Krivovichev, S.V. and Filatov, S.K. (1999) Metal arrays in structural units based on anion-centered metal tetrahedra. *Acta Crystallographica*, **B55**, 664–676.

Krivovichev, S.V., Turner, R., Rumsey, M.S., Siidra, O.I. and Kirk, C.A. (2009) The crystal structure and chemistry of mereheadite. *Mineralogical Magazine*, **73**, 103–117.

Pasero, M. and Vacchiano, D. Crystal structure of mendipite, $Pb_3O_2Cl_2$. *Neues Jahrbuch für Mineralogie*, *Monatshefte*, **2000**, 563–569.

Rumsey, M.S. (2008) The first British occurrence of kombatite; $Pb_{14}[O_9(VO_4)_2Cl_4]$ from the Wesley Mine near Westbury on Trym, Bristol. *Journal of the Russell Society*, **11**, 51–53.

Rumsey, M.S., Krivovichev, S.V., Siidra, O.I., Kirk, C.A., Stanley, C.J. and Spratt, J. (2011) Rickturnerite, $Pb_7O_4[Mg(OH)_4](OH)Cl_3$, a complex new Pb oxychloride mineral. *Mineralogical Magazine*, **76**, 59–73.

Siidra, O.I. and Krivovichev, S.V. (2008) Crystal chemistry of oxocentered lead oxyhalides and their importance as perspective materials. Pp. 129–141 in: *Minerals as Advanced Materials II* (S.V. Krivovichev, editor). Springer, Berlin.

Siidra, O.I., Krivovichev, S.V., Filatov, S.K. (2008*a*) Minerals and synthetic Pb(II) compounds with oxocentered tetrahedra: review and classification. *Zeitschrift für Kristallographie*, **223**, 114–125.

Siidra, O.I., Krivovichev, S.V., Turner, R.W. and Rumsey, M.S. (2008*b*) Chloroxiphite $Pb_3CuO_2(OH)_2Cl_2$ structure refinement and description in terms of oxocentered OPb_4 tetrahedra. *Mineralogical Magazine*, **72**, 793–798.

Siidra, O.I., Krivovichev, S.V., Turner, R.W. and Rumsey, M.S. (2011) Natural and synthetic layered Pb(II) oxyhalides. Pp. 319–332 in: *Minerals as Advanced Materials II* (S.V. Krivovichev, editor). Springer, Berlin.

Turner, R.W. (2006) A mechanism for the formation of the mineralized manganese deposits at Merehead Quarry, Cranmore, Somerset, England.

Mineralogical Magazine, **70**, 629–653.

Turner, R.W. and Rumsey, M.S. (2010) Mineral relationships in the Mendip Hills. *Journal of the Russell Society*, **13**, 3–47.

Turner, R.W., Siidra, O.I., Rumsey, M.S., Krivovichev, S.V., Stanley, C.S. and Spratt, J. (2012). Hereroite and vladkrivovichevite: two novel lead oxychlorides from the Kombat mine, Namibia. *Mineralogical Magazine*, **76**, 883–890.

Welch, M.D., Criddle, A.J. and Symes, R.F. (1998) Mereheadite, $Pb_2O(OH)Cl$: a new litharge-related oxychloride from Merehead Quarry, Cranmore, Somerset. *Mineralogical Magazine*, **62**, 387–393.

```
data_pbfocl

_audit_creation_method            SHELXL-97
_chemical_name_systematic
;
 ?
;
_chemical_name_common             ?
_chemical_melting_point           ?
_chemical_formula_moiety          ?
_chemical_formula_sum
 'Cl2 F2 O2 Pb4'
_chemical_formula_weight          969.66

loop_
 _atom_type_symbol
 _atom_type_description
 _atom_type_scat_dispersion_real
 _atom_type_scat_dispersion_imag
 _atom_type_scat_source
 'Cl'  'Cl'   0.1484   0.1585
 'International Tables Vol C Tables 4.2.6.8 and 6.1.1.4'
 'O'  'O'   0.0106   0.0060
 'International Tables Vol C Tables 4.2.6.8 and 6.1.1.4'
 'Pb'  'Pb'  -3.3944  10.1111
 'International Tables Vol C Tables 4.2.6.8 and 6.1.1.4'
 'F'  'F'   0.0171   0.0103
 'International Tables Vol C Tables 4.2.6.8 and 6.1.1.4'

_symmetry_cell_setting            ?
_symmetry_space_group_name_H-M    ?

loop_
 _symmetry_equiv_pos_as_xyz
 'x, y, z'
 'x, -y, -z'
 '-x, -y, z'
 '-x, y, -z'
 'y, x, -z'
 'y, -x, z'
 '-y, x, z'
 '-y, -x, -z'
 'x+1/2, y+1/2, z+1/2'
 'x+1/2, -y+1/2, -z+1/2'
 '-x+1/2, -y+1/2, z+1/2'
 '-x+1/2, y+1/2, -z+1/2'
 'y+1/2, x+1/2, -z+1/2'
 'y+1/2, -x+1/2, z+1/2'
 '-y+1/2, x+1/2, z+1/2'
 '-y+1/2, -x+1/2, -z+1/2'
 '-x, -y, -z'
 '-x, y, z'
 'x, y, -z'
 'x, -y, z'
 '-y, -x, z'
 '-y, x, -z'
 'y, -x, -z'
 'y, x, z'
 '-x+1/2, -y+1/2, -z+1/2'
```

```
 '-x+1/2, y+1/2, z+1/2'
 'x+1/2, y+1/2, -z+1/2'
 'x+1/2, -y+1/2, z+1/2'
 '-y+1/2, -x+1/2, z+1/2'
 '-y+1/2, x+1/2, -z+1/2'
 'y+1/2, -x+1/2, -z+1/2'
 'y+1/2, x+1/2, z+1/2'

_cell_length_a                    4.0648(19)
_cell_length_b                    4.0648(19)
_cell_length_c                    12.631(7)
_cell_angle_alpha                 90.00
_cell_angle_beta                  90.00
_cell_angle_gamma                 90.00
_cell_volume                      208.70(18)
_cell_formula_units_Z             1
_cell_measurement_temperature     293(2)
_cell_measurement_reflns_used     ?
_cell_measurement_theta_min       ?
_cell_measurement_theta_max       ?

_exptl_crystal_description        ?
_exptl_crystal_colour             ?
_exptl_crystal_size_max           ?
_exptl_crystal_size_mid           ?
_exptl_crystal_size_min           ?
_exptl_crystal_density_meas       ?
_exptl_crystal_density_diffrn     7.715
_exptl_crystal_density_method     'not measured'
_exptl_crystal_F_000              396
_exptl_absorpt_coefficient_mu     81.038
_exptl_absorpt_correction_type    ?
_exptl_absorpt_correction_T_min   ?
_exptl_absorpt_correction_T_max   ?
_exptl_absorpt_process_details    ?

_exptl_special_details
;
 ?
;

_diffrn_ambient_temperature       293(2)
_diffrn_radiation_wavelength      0.71073
_diffrn_radiation_type            MoK\a
_diffrn_radiation_source          'fine-focus sealed tube'
_diffrn_radiation_monochromator   graphite
_diffrn_measurement_device_type   ?
_diffrn_measurement_method        ?
_diffrn_detector_area_resol_mean  ?
_diffrn_standards_number          ?
_diffrn_standards_interval_count  ?
_diffrn_standards_interval_time   ?
_diffrn_standards_decay_%         ?
_diffrn_reflns_number             93
_diffrn_reflns_av_R_equivalents   0.0000
_diffrn_reflns_av_sigmaI/netI     0.0651
_diffrn_reflns_limit_h_min        0
_diffrn_reflns_limit_h_max        3
_diffrn_reflns_limit_k_min        0
_diffrn_reflns_limit_k_max        5
_diffrn_reflns_limit_l_min        0
```

```
_diffrn_reflns_limit_l_max        16
_diffrn_reflns_theta_min          6.98
_diffrn_reflns_theta_max          27.83
_reflns_number_total              93
_reflns_number_gt                 64
_reflns_threshold_expression      >2sigma(I)

_computing_data_collection        ?
_computing_cell_refinement        ?
_computing_data_reduction         ?
_computing_structure_solution     ?
_computing_structure_refinement   'SHELXL-97 (Sheldrick, 1997)'
_computing_molecular_graphics     ?
_computing_publication_material   ?

_refine_special_details
;
 Refinement of F^2^ against ALL reflections.  The weighted R-factor wR and
 goodness of fit S are based on F^2^, conventional R-factors R are based
 on F, with F set to zero for negative F^2^. The threshold expression of
 F^2^ > 2sigma(F^2^) is used only for calculating R-factors(gt) etc. and is
 not relevant to the choice of reflections for refinement.  R-factors based
 on F^2^ are statistically about twice as large as those based on F, and R-
 factors based on ALL data will be even larger.
;

_refine_ls_structure_factor_coef  Fsqd
_refine_ls_matrix_type            full
_refine_ls_weighting_scheme       calc
_refine_ls_weighting_details
 'calc w=1/[\s^2^(Fo^2^)+(0.1323P)^2^+0.0000P] where P=(Fo^2^+2Fc^2^)/3'
_atom_sites_solution_primary      direct
_atom_sites_solution_secondary    difmap
_atom_sites_solution_hydrogens    geom
_refine_ls_hydrogen_treatment     mixed
_refine_ls_extinction_method      SHELXL
_refine_ls_extinction_coef        0.003(5)
_refine_ls_extinction_expression
 'Fc^*^=kFc[1+0.001xFc^2^\l^3^/sin(2\q)]^-1/4^'
_refine_ls_number_reflns          93
_refine_ls_number_parameters      9
_refine_ls_number_restraints      0
_refine_ls_R_factor_all           0.0993
_refine_ls_R_factor_gt            0.0709
_refine_ls_wR_factor_ref          0.2148
_refine_ls_wR_factor_gt           0.2023
_refine_ls_goodness_of_fit_ref    1.107
_refine_ls_restrained_S_all       1.107
_refine_ls_shift/su_max           0.000
_refine_ls_shift/su_mean          0.000

loop_
 _atom_site_label
 _atom_site_type_symbol
 _atom_site_fract_x
 _atom_site_fract_y
 _atom_site_fract_z
 _atom_site_U_iso_or_equiv
 _atom_site_adp_type
 _atom_site_occupancy
 _atom_site_symmetry_multiplicity
```

```
 _atom_site_calc_flag
 _atom_site_refinement_flags
 _atom_site_disorder_assembly
 _atom_site_disorder_group
Pb1 Pb 0.0000 0.0000 0.1469(3) 0.061(2) Uani 1 8 d S . .
Cl1 Cl 0.5000 0.5000 0.0000 0.056(7) Uani 1 16 d S . .
O1 O -0.5000 0.0000 0.2500 0.049(11) Uani 0.50 8 d SP . .
F1 F -0.5000 0.0000 0.2500 0.049(11) Uani 0.50 8 d SP . .

loop_
 _atom_site_aniso_label
 _atom_site_aniso_U_11
 _atom_site_aniso_U_22
 _atom_site_aniso_U_33
 _atom_site_aniso_U_23
 _atom_site_aniso_U_13
 _atom_site_aniso_U_12
Pb1 0.065(2) 0.065(2) 0.052(2) 0.000 0.000 0.000
Cl1 0.062(11) 0.062(11) 0.043(14) 0.000 0.000 0.000
O1 0.049(17) 0.049(17) 0.05(2) 0.000 0.000 0.000
F1 0.049(17) 0.049(17) 0.05(2) 0.000 0.000 0.000

_geom_special_details
;
 All esds (except the esd in the dihedral angle between two l.s. planes)
 are estimated using the full covariance matrix.  The cell esds are taken
 into account individually in the estimation of esds in distances, angles
 and torsion angles; correlations between esds in cell parameters are only
 used when they are defined by crystal symmetry.  An approximate (isotropic)
 treatment of cell esds is used for estimating esds involving l.s. planes.
;

loop_
 _geom_bond_atom_site_label_1
 _geom_bond_atom_site_label_2
 _geom_bond_distance
 _geom_bond_site_symmetry_2
 _geom_bond_publ_flag
Pb1 F1 2.414(2) 25_455 ?
Pb1 F1 2.414(2) 1_655 ?
Pb1 O1 2.414(2) 25_455 ?
Pb1 O1 2.414(2) 1_655 ?
Pb1 F1 2.414(2) 25_445 ?
Pb1 O1 2.414(2) . ?
Pb1 O1 2.414(2) 25_445 ?
Pb1 Cl1 3.421(2) 1_445 ?
Pb1 Cl1 3.421(2) . ?
Pb1 Cl1 3.421(2) 1_455 ?
Pb1 Cl1 3.421(2) 1_545 ?
Cl1 Pb1 3.421(2) 17 ?
Cl1 Pb1 3.421(2) 1_665 ?
Cl1 Pb1 3.421(2) 17_665 ?
Cl1 Pb1 3.421(2) 1_655 ?
Cl1 Pb1 3.421(2) 1_565 ?
Cl1 Pb1 3.421(2) 17_655 ?
Cl1 Pb1 3.421(2) 17_565 ?
O1 Pb1 2.414(2) 25_455 ?
O1 Pb1 2.414(2) 1_455 ?
O1 Pb1 2.414(2) 25_445 ?

loop_
```

```
 _geom_angle_atom_site_label_1
 _geom_angle_atom_site_label_2
 _geom_angle_atom_site_label_3
 _geom_angle
 _geom_angle_site_symmetry_1
 _geom_angle_site_symmetry_3
 _geom_angle_publ_flag
F1 Pb1 F1 73.08(7) 25_455 1_655 ?
F1 Pb1 O1 0.0 25_455 25_455 ?
F1 Pb1 O1 73.08(7) 1_655 25_455 ?
F1 Pb1 O1 73.08(7) 25_455 1_655 ?
F1 Pb1 O1 0.0 1_655 1_655 ?
O1 Pb1 O1 73.08(7) 25_455 1_655 ?
F1 Pb1 F1 114.71(16) 25_455 25_445 ?
F1 Pb1 F1 73.08(7) 1_655 25_445 ?
O1 Pb1 F1 114.71(16) 25_455 25_445 ?
O1 Pb1 F1 73.08(7) 1_655 25_445 ?
F1 Pb1 O1 73.08(7) 25_455 . ?
F1 Pb1 O1 114.71(16) 1_655 . ?
O1 Pb1 O1 73.08(7) 25_455 . ?
O1 Pb1 O1 114.71(16) 1_655 . ?
F1 Pb1 O1 73.08(7) 25_445 . ?
F1 Pb1 O1 114.71(16) 25_455 25_445 ?
F1 Pb1 O1 73.08(7) 1_655 25_445 ?
O1 Pb1 O1 114.71(16) 25_455 25_445 ?
O1 Pb1 O1 73.08(7) 1_655 25_445 ?
F1 Pb1 O1 0.0 25_445 25_445 ?
O1 Pb1 O1 73.08(7) . 25_445 ?
F1 Pb1 Cl1 142.448(10) 25_455 1_445 ?
F1 Pb1 Cl1 142.448(10) 1_655 1_445 ?
O1 Pb1 Cl1 142.448(10) 25_455 1_445 ?
O1 Pb1 Cl1 142.448(10) 1_655 1_445 ?
F1 Pb1 Cl1 78.02(4) 25_445 1_445 ?
O1 Pb1 Cl1 78.02(4) . 1_445 ?
O1 Pb1 Cl1 78.02(4) 25_445 1_445 ?
F1 Pb1 Cl1 78.02(4) 25_455 . ?
F1 Pb1 Cl1 78.02(4) 1_655 . ?
O1 Pb1 Cl1 78.02(4) 25_455 . ?
O1 Pb1 Cl1 78.02(4) 1_655 . ?
F1 Pb1 Cl1 142.448(10) 25_445 . ?
O1 Pb1 Cl1 142.448(10) . . ?
O1 Pb1 Cl1 142.448(10) 25_445 . ?
Cl1 Pb1 Cl1 114.30(11) 1_445 . ?
F1 Pb1 Cl1 78.02(4) 25_455 1_455 ?
F1 Pb1 Cl1 142.448(10) 1_655 1_455 ?
O1 Pb1 Cl1 78.02(4) 25_455 1_455 ?
O1 Pb1 Cl1 142.448(10) 1_655 1_455 ?
F1 Pb1 Cl1 142.448(10) 25_445 1_455 ?
O1 Pb1 Cl1 78.02(4) . 1_455 ?
O1 Pb1 Cl1 142.448(10) 25_445 1_455 ?
Cl1 Pb1 Cl1 72.89(5) 1_445 1_455 ?
Cl1 Pb1 Cl1 72.89(5) . 1_455 ?
F1 Pb1 Cl1 142.448(10) 25_455 1_545 ?
F1 Pb1 Cl1 78.02(4) 1_655 1_545 ?
O1 Pb1 Cl1 142.448(10) 25_455 1_545 ?
O1 Pb1 Cl1 78.02(4) 1_655 1_545 ?
F1 Pb1 Cl1 78.02(4) 25_445 1_545 ?
O1 Pb1 Cl1 142.448(10) . 1_545 ?
O1 Pb1 Cl1 78.02(4) 25_445 1_545 ?
Cl1 Pb1 Cl1 72.89(5) 1_445 1_545 ?
Cl1 Pb1 Cl1 72.89(5) . 1_545 ?
```

```
Cl1 Pb1 Cl1 114.30(11) 1_455 1_545 ?
Pb1 Cl1 Pb1 180.00(11) 17 1_665 ?
Pb1 Cl1 Pb1 65.70(11) 17 . ?
Pb1 Cl1 Pb1 114.30(11) 1_665 . ?
Pb1 Cl1 Pb1 114.30(11) 17 17_665 ?
Pb1 Cl1 Pb1 65.70(11) 1_665 17_665 ?
Pb1 Cl1 Pb1 180.00(11) . 17_665 ?
Pb1 Cl1 Pb1 107.11(5) 17 1_655 ?
Pb1 Cl1 Pb1 72.89(5) 1_665 1_655 ?
Pb1 Cl1 Pb1 72.89(5) . 1_655 ?
Pb1 Cl1 Pb1 107.11(5) 17_665 1_655 ?
Pb1 Cl1 Pb1 107.11(5) 17 1_565 ?
Pb1 Cl1 Pb1 72.89(5) 1_665 1_565 ?
Pb1 Cl1 Pb1 72.89(5) . 1_565 ?
Pb1 Cl1 Pb1 107.11(5) 17_665 1_565 ?
Pb1 Cl1 Pb1 114.30(11) 1_655 1_565 ?
Pb1 Cl1 Pb1 72.89(5) 17 17_655 ?
Pb1 Cl1 Pb1 107.11(5) 1_665 17_655 ?
Pb1 Cl1 Pb1 107.11(5) . 17_655 ?
Pb1 Cl1 Pb1 72.89(5) 17_665 17_655 ?
Pb1 Cl1 Pb1 65.70(11) 1_655 17_655 ?
Pb1 Cl1 Pb1 180.0 1_565 17_655 ?
Pb1 Cl1 Pb1 72.89(5) 17 17_565 ?
Pb1 Cl1 Pb1 107.11(5) 1_665 17_565 ?
Pb1 Cl1 Pb1 107.11(5) . 17_565 ?
Pb1 Cl1 Pb1 72.89(5) 17_665 17_565 ?
Pb1 Cl1 Pb1 180.00(11) 1_655 17_565 ?
Pb1 Cl1 Pb1 65.70(11) 1_565 17_565 ?
Pb1 Cl1 Pb1 114.30(11) 17_655 17_565 ?
Pb1 O1 Pb1 106.92(7) 25_455 1_455 ?
Pb1 O1 Pb1 114.71(16) 25_455 25_445 ?
Pb1 O1 Pb1 106.92(8) 1_455 25_445 ?
Pb1 O1 Pb1 106.92(8) 25_455 . ?
Pb1 O1 Pb1 114.71(16) 1_455 . ?
Pb1 O1 Pb1 106.92(8) 25_445 . ?

_diffrn_measured_fraction_theta_max    0.930
_diffrn_reflns_theta_full              27.83
_diffrn_measured_fraction_theta_full   0.930
_refine_diff_density_max    2.900
_refine_diff_density_min   -2.366
_refine_diff_density_rms    0.643
```